Electronic signature of the magicity and ionic bonding in $Al_{13}X$ (X=Li–K) clusters

S. N. Khanna, B. K. Rao, and P. Jena
Physics Department, Virginia Commonwealth University, Richmond, Virginia 23284-2000
(Received 16 April 2001; published 12 March 2002)

Total energies and equilibrium geometries of neutral and anionic Al_n and Al_nX ($n=12-14$, $X=$Li, Na, K) clusters have been obtained following an optimization of their structure without any symmetry constraint. The calculations are based on molecular-orbital approach and the gradient-corrected density-functional theory. It is shown that although the binding energy of $Al_{13}X$ clusters do not differ much from that of their neighbors, their ionization potentials, highest occupied molecular orbital and lowest unoccupied molecular orbital gaps, and electron affinities bear distinct signature of their magicity. That the binding of Al_{13} with alkali atoms is predominantly ionic is derived by comparing the electron affinity of $Al_{13}X$ with other known salts.

DOI: 10.1103/PhysRevB.65.125105 PACS number(s): 73.22.−f, 31.15.Ar, 71.15.Nc

I. INTRODUCTION

The discovery of magic numbers in Na_n clusters and the realization that the origin of their enhanced stability is due to electronic shell closure[1] has fueled considerable theoretical and experimental interest in the past two decades. Several studies[2,3] have since been carried out to find other magic clusters by not only varying the size and composition of clusters but also their charge state. Among all the clusters studied, Al_{13}-based clusters constitute the leading group.[4] It was found earlier that Al_{13}^- cluster with its 40 valence electrons is not only very stable but also unreactive in comparison to its neighbors.[5] Later work concentrated on compound metal clusters[6] consisting of $Al_{13}X$, where X is an alkali atom. Since the alkali atoms are monovalent and Al atoms are trivalent, $Al_{13}X$ contains 40 valence electrons and, thus, is expected to be very stable. However, unlike Al_{13}^-, which has the shape of a perfectly symmetric icosahedron, the geometry of $Al_{13}X$ has to be asymmetric since either the alkali atom (X) or one of the Al atoms has to reside outside the icosahedric cage. Thus, $Al_{13}X$ structure would not be as symmetric as other homonuclear magic clusters. This is one of the reasons that has made the proof of the magicity of $Al_{13}X$ a difficult one.

There are, however, electronic signatures of magic clusters that can be explored. Since magic clusters are usually characterized by electronic shell closure, the gap between their highest occupied molecular orbital (HOMO) and lowest unoccupied molecular orbital (LUMO) and ionization potential should be large. In the same vein $Al_{13}X$ clusters should also have low electron affinity. To demonstrate unambiguously that $Al_{13}X$ clusters are magic, one not only has to determine their HOMO-LUMO gaps, ionization potentials, and electron affinities but also compare them with the corresponding quantities for $Al_{12}X$ and $Al_{14}X$ clusters. While these studies of $Al_{13}X$ clusters are available, no such studies are available for the neighboring species.

We have, therefore, studied the equilibrium geometries of Al_nX ($n=12$, 13, 14 and $X=$Li, Na, K) clusters in both neutral and anionic configurations. These studies were prompted by recent experimental investigations[7] of these systems using negative-ion photodetachment spectroscopy. In this paper, we present these results and demonstrate that the electronic structure of $Al_{13}X$ clusters is indeed unique and their low electron affinity, high ionization potential, and large HOMO-LUMO gap place them into the magic class of clusters. In addition, the electron affinities of the $Al_{13}X$ clusters are consistent with other known salts, thus providing unmistakable signature of an ionic bond between Al_{13} and X, alkali atoms. That two metallic elements can bind ionically in the cluster form provides unique opportunities for the synthesis of novel materials where clusters,[8] and not atoms, serve as building blocks.

In the following, we briefly discuss our computational method. The results are presented in Sec. III and summarized in Sec. IV.

II. COMPUTATIONAL DETAILS

The calculations are carried out at the first-principles level by using the molecular-orbital approach and the density-functional theory (DFT). The molecular orbitals were formed from a linear combination of Gaussian functions centered at the atomic sites and the exchange correlation effects are included via a gradient-corrected density-functional proposed by Perdew, Burke, and Ernzerhof.[9] All the calculations are done at the all electron level.

The actual computations were carried out using a set of programs called NRLMOL that were developed by Pederson and Jackson.[10] Here the integrals required in the solutions of the Kohn-Sham equations are carried out numerically over a mesh of points. The basis sets consisted of $6s$, $5p$, and $3d$ functions with an auxiliary d function for Al; $5s$, $3p$, and $1d$ with 1 auxiliary p and 1 auxiliary d functions for Li; $6s$, $4p$, and $3d$ functions with an auxiliary d function for Na; and a $7s$, $5p$, and $3d$ functions with an auxiliary d function for K. These were built by contracting a set of 16 primitive Gaussians in the case of Al, 10 for Li, 16 for Na, and 17 for K. As to the details of the basis sets, the reader is referred to earlier papers.[11] It should be pointed out that this basis set is large enough with sufficient diffuse functions to describe negative cluster ions that have delocalized electrons. This confidence results from the agreement between the calculated and the experimental electron affinities. For each cluster, the geometry was optimized by moving atoms in the direction of forces till the forces were lower than the threshold value of 3.0×10^{-4} a.u./bohr. As mentioned before, no symmetry

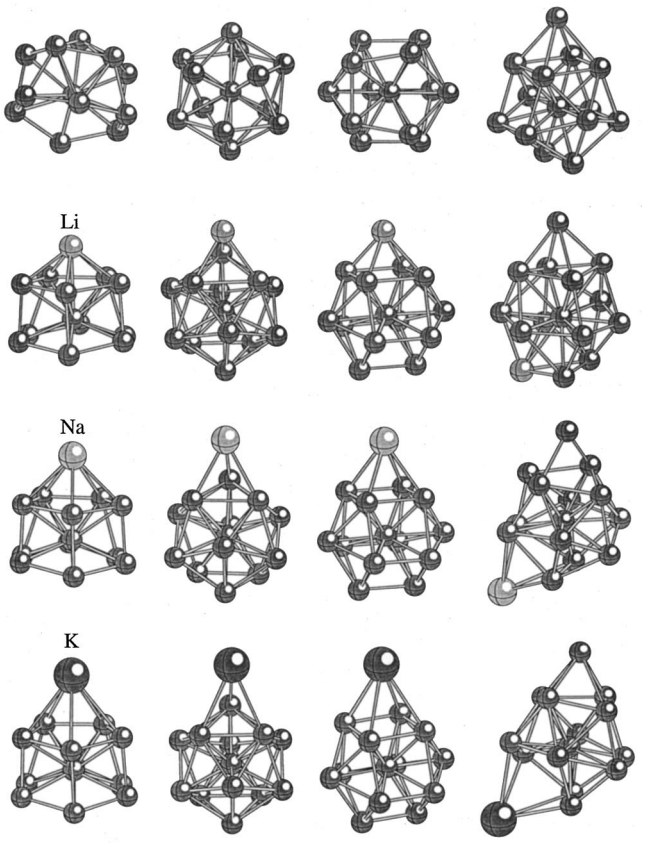

FIG. 1. Ground-state geometries of Al_n, Al_nLi, Al_nNa, and Al_nK ($n=12-14$) clusters. For the 13-atom clusters, the icosahedric and the decahedral isomers are shown. Column 1–4 correspond to Al_{12}, Al_{13}-ico, Al_{13}-deca, and Al_{14} while the row 1–4 correspond to pure, Li, Na, and K attached to Al_n clusters.

constraints were imposed and the optimized structures include possible Jahn-Teller distortions.

III. RESULTS

A. Geometry and energetic stability

Numerous theoretical calculations on the equilibrium geometries, binding energies, and ionization potentials of Al_n clusters $n \leqslant 14$ using various levels of approximations are available in the literature and the reader is referred to earlier papers for comparison.[12] Here we wish to focus on the effect of alkali atoms (X) on the electronic structure and stability of Al_nX clusters for $n=12$, 13, and 14. To this end we show in Fig. 1, the ground-state geometries of the pure and doped clusters. In Table I we give the total energies of Al_n and Al_nX ($n=12-14$) clusters corresponding to their optimized geometries. We define these energies as

$$E_b = -[E(\mathrm{Al}_n) - nE(\mathrm{Al})]/n \tag{1}$$

for pure clusters and

$$E_b = -[E(\mathrm{Al}_nX) - nE(\mathrm{Al}) - E(X)]/(n+1) \tag{2}$$

for mixed clusters. Here $E(\mathrm{Al}_n)$ and $E(\mathrm{Al}_nX)$ are the total energies of the Al_n, and Al_nX clusters, respectively. Note

TABLE I. Binding energy per atom (eV), of pure and doped Al_{12}, Al_{13}, and Al_{14} clusters.

	Cluster			
X	Al_{12}-X	Al_{13} (ico)-X	Al_{13} (dec)-X	Al_{14}-X
Bare	2.47	2.70	2.67	2.60
Li	2.45	2.60	2.58	2.54
Na	2.40	2.57	2.55	2.53
K	2.41	2.58	2.55	2.52

that Al_{12} is a closed structure, while Al_{13} is characterized by two isomers in the form of an icosahedron and decahedron. The icosahedron ground state is only 0.23 eV (total energy) more stable than the decahedral structure and we had earlier shown[13] that the observed negative-ion photoelectron spectra on Al_{13}^- agrees with the icosahedral structure. We would like to add that the lowering of the energy of the distorted icosahedron or decahedron from the perfect icosahedral structure is caused by the relaxation of the surface strain. In a perfect icosahedron the surface bonds are 5% longer than the radial bonds and there are 30 surface bonds and 12 radial bonds. We found that the distortion in icosahedron leads to a narrower distribution of bond distances among all the atoms. The strain can be further reduced by going to decahedron but this also leads to a reduction in the number of bonds. We found that while the two structures are close in energy, it is the icosahedron that is slightly more stable. The structure of Al_{14} can be described as an Al_{13} icosahedron with a face capped by an Al atom.

The addition of alkali atoms leads to a significant rearrangement of atoms for the Al_{12} cluster. For bigger sizes, the alkali atoms decorate the faces without much distorting the structure. Also, as the sizes of the alkali atoms increase, the distance of the alkali from the Al cluster cage increases.

From Table I we note that Al_{13} has the highest binding energy per atom. The gain in binding energy is higher in going from 12 to 13 than the loss in going from 13 to 14. Since none of the cluster sizes corresponds to a completely filled electronic shell, the increase from 12 to 13 is indicative of the geometrical shell closure. Intriguingly, this trend is unchanged as an alkali atom is added to the cluster even though $Al_{12}X$ has enough atoms to close a geometrical shell. The reason for this behavior lies in the nature of the electronic coupling. As we will show, the Al_n clusters have high electron affinities and their coupling to an alkali atom is primarily ionic in nature. The addition of an alkali atom to Al_{12} then does not lead to a geometrically compact structure, as the ionic bond tends to distort the noncompact pure Al_n structure. The compact structures emerge for the 13-atom cluster. Even more intriguing is the fact that the gain in binding energy of Al_{13} clusters with the addition of an Al or alkali is almost the same. This is surprising since Al and K are immiscible in the liquid form and show a special electronic bonding mechanism between the Al_{13} and the alkali atoms. We also note that the binding energy per atom of Al_nX clusters defined in Eq. (2) remain essentially the same for all the alkali atoms, X. This implies that the nature of bonding between X and Al_n remains unchanged in going from Li to K.

B. HOMO-LUMO gap, electron affinity, and the ionization potential

To investigate these electronic effects and the corresponding shell closure in detail one has to study the behavior of the clusters upon the addition or removal of a single electron. We have, therefore, carried out calculations of the corresponding anionic and cationic clusters. The HOMO-LUMO gap, vertical-electron detachment energy (VDE), the adiabatic electron affinity (AEA) as well as the vertical ionization potential (VIP) were calculated. VDE is the difference between the ground-state energy of the anion and that of the neutral cluster having the anionic geometry. AEA, on the other hand, is the difference in ground-state energies of the anionic and the neutral clusters. The VDE is always larger than the AEA and the difference between the two is a measure of the energy gain due to structural relaxation. As pointed out, some of these quantities have been recently measured[7] and, therefore, one can compare the theoretical predictions against these measurements.

In Fig. 2 we show the VIP, the HOMO-LUMO gap and AEA of pure and alkali-doped clusters. We start with the ionization potential first. Note that the pure clusters have higher ionization potentials than the alkali-doped clusters. The ionization potential for the 13-atom clusters is higher than for the 12- and 14-atom clusters. For the pure clusters, the Al_{12}, Al_{13}, and Al_{14} have 36, 39, and 42 valence electrons, respectively. Starting from Al_{12}, as one goes to Al_{13}, one is approaching the shell closure of 40 electrons. Removal of an electron takes us away from the shell closure. Consequently, Al_{13} has a higher VIP than Al_{12} since the parent is closer to the shell closure. The situation changes for Al_{14} where the ionized cluster is closer to the shell filling than the parent and it has the lowest VIP. Addition of an alkali atom to the pure cluster changes the electron count by one but the trend is identical. Note that the alkali atoms have lower IP and this leads to the lowering of the VIP when an alkali is added.

While the ionization does bring out electronic features, the shell closure is most transparent in the HOMO-LUMO gap and the AEA. These are shown in Fig. 2. Let us start with HOMO-LUMO gap first. An Al_{13}^- has 40 valence electrons whereas both Al_{12}^- and Al_{14}^- are, respectively, three electrons shy and three electrons above the shell closure. The shell closure makes Al_{13}^- as the most stable cluster with the highest HOMO-LUMO gap of 1.87 eV, while Al_{12}^- and Al_{14}^- have significantly lower HOMO-LUMO gaps of 0.17 and 0.44 eV, respectively. Note that the AEA of Al_{13} is comparable to 3.36 eV for Br and, therefore, it behaves like a halogen atom. One can, therefore, form ionic ''molecules'' by combining Al_{13} with alkali atoms. The extra electron from the alkali atom leads to a shell closure only in $Al_{13}X$. This makes $Al_{13}X^-$ as a less stable cluster and indeed the AEA has a sharp dip for the $Al_{13}X$ cluster as opposed to the peak for the pure clusters. In our view, this is the most vivid demonstration of the shell closure.

Bowen and co-workers[7] have recently carried out the negative-ion photoelectron spectroscopy experiments on Al_nLi and Al_nK clusters. In these experiments, one starts

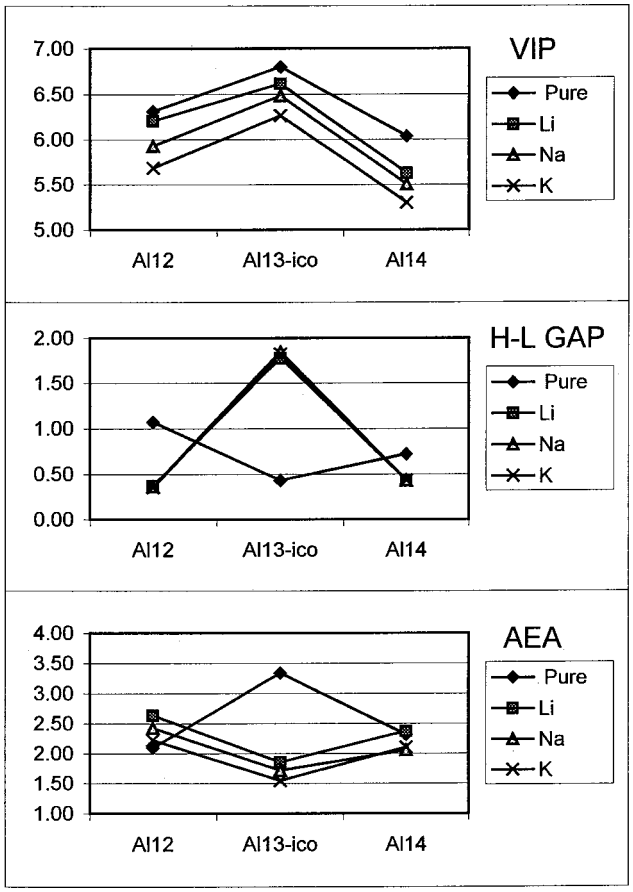

FIG. 2. Vertical ionization potential (VIP), HOMO-LUMO gap (H-L gap), and adiabatic electron affinity (AEA) in Al_{12}, Al_{13}-ico, and Al_{14} clusters. All energies are in eV.

with the size selected clusters and provides excess energy via photons of fixed frequency that will detach electrons. The energy of the detached electrons can provide direct information on the vertical transitions from the anion to the neutral configurations of various spins. While these experiments are currently underway, their preliminary investigations on Al_nLi clusters indicate that the photoelectron spectra of $Al_{13}Li$ is marked by peaks around 2.1 and 3.1 eV. Starting from our calculated ground state of the anion, we find the vertical transition energies to the neutral singlet and triplet states to be 2.05 and 3.30 eV, respectively which are close to the experimental values. For the $Al_{13}K^-$, their preliminary spectra indicate peaks around 1.9, 2.4, and 3.1 eV. Our calculated transitions to singlet and triplet states occur at 1.75 and 3.04 eV, respectively. We are unable to account for the peak around 2.4 eV. These experiments also indicate a dip in the electron affinity at $Al_{13}Li$ and $Al_{13}K$ as predicted by the present investigations. Note that these experimental results are only preliminary, and a detailed comparison will be reported later.

In order to further justify that the electron affinity anomaly observed in $Al_{13}X$ clusters is characteristic of an ionically bonded salt, we recall the work by Miller *et al.*[14] They have made a systematic analysis of the electron affinities (EA) of many alkali-halide molecules that are characterized by ionic bonding. They had shown that the EA (in eV)

follows a simple empirical rule, i.e., $EA = 1.189 - 0.103\,\alpha_M / r_{MX}^2$ where α_M is the polarizability of the alkali atom and r_{MX} is the neutral molecular equilibrium bond length. This puts a limit of 1.2 eV on the EA of a salt. The computed electron affinity of $Al_{13}Li$, $Al_{13}Na$, and $Al_{13}K$ are 1.85, 1.71, and 1.54 eV, respectively. Note that with increasing size of the alkali atom, the EA of $Al_{13}X$ approaches the limiting value of 1.2 eV.

C. Electronic structure and charge density distribution in Al_{13}, $Al_{13}K$, and Al_{14} clusters

It is instructive to reconfirm the electronic structure of Al_{13}-based clusters by analyzing the electron charge density distribution. We have plotted the isodensity surfaces in Fig. 3 for Al_{13}, $Al_{13}K$, and Al_{14} clusters. Note that the bonding between Al atoms in all of these clusters is evident from the overlap of electron density from neighboring sites. The situation is rather unique for $Al_{13}K$. Here the charge density of the K atom remains almost spherical and there is very little electron-density overlap between K and Al_{13}. This is characteristic of an ionic bond. Note that for Al_{14} cluster, which essentially has the same geometry as $Al_{13}K$, there is significant electron-density overlap between the 14th Al atom and Al_{13} cluster. The Mulliken charge distribution also reflects this behavior. The K atom essentially remains as a positive ion with a Mulliken charge of 0.74 while the Al_{13} cage carries the negative charge. This type of behavior is noticed for the interaction of all the alkali atoms with the Al_{13} cluster.

Further evidence of the ionic bonding between Al_{13} and the alkali atom (X) can be found from an analysis of the dipole moments of $Al_{13}X$ clusters. In the Al_{13} cluster, the central Al atom carries a slight extra amount of Mulliken charge while the outer shell is slightly positive.[15] When an alkali atom (X) with a positive Mulliken charge is added to this, one expects a dipole moment associated with the resulting ionic bonding. Our results for dipole moments of $Al_{13}X$ are 3.50, 6.67, and 11.18 D for Li, Na, and K, respectively. Clearly the ionicity of the bonding is increasing from Li to K. For $Al_{13}X^-$ clusters, the values of the dipole moments are expected to decrease because the additional electron would cause the loss of the positive Mulliken charge at the alkali-atom site. We find that $Al_{13}Li^-$ and $Al_{13}K^-$ have dipole moments of 2.69 and 10.48 D, respectively. The ionic nature of the bonding is thus established.

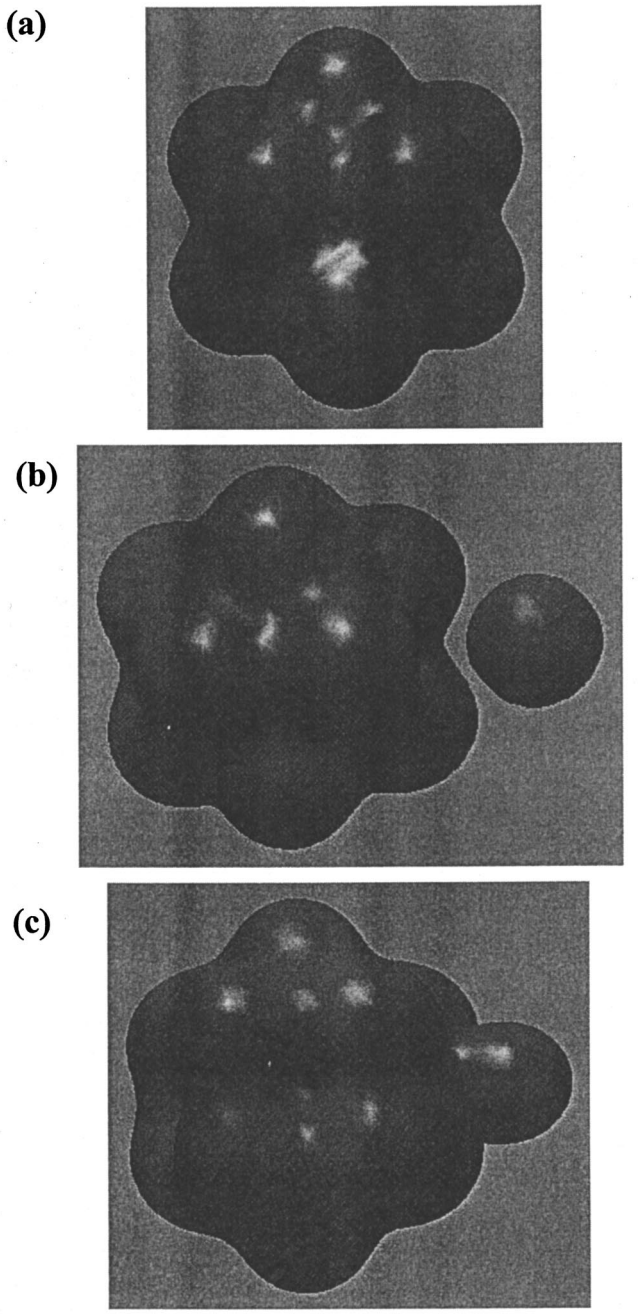

FIG. 3. Isodensity surfaces for charge-density distribution in (a) Al_{13}, (b) $Al_{13}K$, and (c) Al_{14} clusters.

IV. CONCLUSIONS

Ab initio calculations based on generalized gradient approximation to the density-functional theory have been carried out to probe the relativity stability, electronic structure, ionization potential, and EA of Al_nX ($n = 12-14$) clusters and compared with those of Al_n in the same size range. The large HUMO-LUMO gap and large ionization potential of $Al_{13}X$ clusters compared to their neighbors are characteristic of electronic shell structure. However, the ionic interaction that binds Al_{13} to X (alkali atoms) is evident from studies of their adiabatic electron affinity. While the AEA of Al_{13} is the largest among Al_n clusters studied, it is the smallest for $Al_{13}X$. This behavior is consistent with the characteristics of known salts surveyed by Miller *et al.*[14] That the AEA of $Al_{13}X$ ranges between 1.5–1.7 eV and are substantially less than that of Al_{13} testifies to the unique chemistry of $Al_{13}X$ clusters.

ACKNOWLEDGMENT

This work is supported by a grant from the Department of Energy (DEFG05-87E61316). The authors are thankful to Professor K. H. Bowen for his sharing of experimental data before publications and for fruitful discussions.

[1] W. D. Knight, K. Clemenger, W. A. de Heer, W. A. Saunders, M. Y. Chou, and M. L. Cohen, Phys. Rev. Lett. **52**, 2141 (1984).
[2] M. M. Kappes, R. Kunz, and E. Schumacher, Chem. Phys. Lett. **119**, 11 (1985).
[3] M. P. Iniguez, J. A. Alanso, A. Rubio, M. J. Lopez, and L. C. Basbas, Phys. Rev. B **41**, 5595 (1990).
[4] S. N. Khann and P. Jena, Phys. Rev. Lett. **69**, 1664 (1992); A. P. Seitsonen, M. J. Puska, M. Alatalo, R. M. Nieminen, V. Milman, and M. C. Payne, Phys. Rev. B **48**, 1981 (1993); X. G. Gong, *ibid.* **56**, 1091 (1997).
[5] R. E. Leuchtner, A. C. Harms, and A. W. Castleman, Jr., J. Chem. Phys. **91**, 2753 (1989).
[6] S. N. Khanna and P. Jena, Chem. Phys. Lett. **219**, 479 (1994).
[7] K. H. Bowen (Private Communication).
[8] S. N. Khanna and P. Jena, Phys. Rev. B **51**, 13 705 (1995); F. Liu, M. Mostoller, T. Kaplan, S. N. Khanna, and P. Jena, Chem. Phys. Lett. **248**, 213 (1996).
[9] J. P. Perdew, K. Burke, and M. Ernzerhof, Phys. Rev. Lett. **77**, 3865 (1996).
[10] M. R. Pederson and K. A. Jackson, Phys. Rev. B **41**, 7453 (1990); K. A. Jackson and M. R. Pederson, *ibid.* **42**, 3276 (1990).
[11] D. V. Porezag and M. R. Pederson, Phys. Rev. A **60**, 2840 (1999).
[12] B. K. Rao and P. Jena, J. Chem. Phys. **111**, 1890 (1999) and references therein.
[13] C. Ashman, S. N. Khanna, J. Kortus, and M. R. Pederson, in *Cluster and Nanostructure Interfaces* edited by P. Jena, S. N. Khanna, and B. K. Rao (World Scientific, Singapore, 2000), p. 383.
[14] T. M. Miller, D. G. Leopold, K. M. Murray, and W. C. Lineberger, J. Chem. Phys. **85**, 2368 (1986).
[15] B. K. Rao, S. N. Khanna, and P. Jena, Phys. Rev. B **62**, 4666 (2000).